

Thermal kinetics study and flammability evaluation of polyimide fiber material

Fanglong Zhu¹ · Yanfang Xu² · Qianqian Feng¹ · Qiuyue Yang¹

Received: 24 June 2017 / Accepted: 27 September 2017 / Published online: 16 October 2017
© Akadémiai Kiadó, Budapest, Hungary 2017

Abstract The thermal stability and flammability of polyimide (PI) fiber for fire protection applications have been assessed by dynamic thermogravimetry and microscale combustion calorimetry (MCC) measurements, respectively. The polymer decomposed in a single step and main pyrolysis occurs within a very narrow temperature range. The kinetic analysis of the main pyrolysis process was conducted by a composite procedure involving the iso-conversional method and the Master-plots method. The main process reaction mechanism of the polyimide obeyed random nucleation model with three nuclei on the individual particle. Compared with polysulfonamide fiber and Meta-aramid (NOMEX 1313) inherently heat-resistant fiber, flammability evaluation from LOI values and MCC data indicated that PI fiber exhibited lower flammability in terms of the ability to ignite and higher flammability in terms of the heat release capacity during combustion. This analysis for kinetics of the PI fiber is useful information for further study of numerical simulation of pyrolysis process of PI fabric when exposed to intense heat flux.

Keywords Thermal stability · Thermal degradation · Thermogravimetric · Kinetic · Polyimide

Introduction

Because of their outstanding thermal and mechanical stability, heat and chemical-resistant properties, aromatic polyimides have become attractive polymeric materials for uses in a wide variety of demanding high-temperature applications, such as hot gas filters for removal of PM 2.5 particles, aircraft components and firefighters' protective clothing [1–3]. All these applications took the advantages of their inflammability and thermal stability. When these polyimide materials are exposed to high heat flux (fire scene), they will experience decomposition or char formation because of their lower melting or pyrolysis temperature than encountering temperature, which can reach up to 800 °C under fire [4]. This will alter the thermal properties of polyimide fabrics. Therefore, some researchers have synthesized different polyimide materials containing various units and evaluated their pyrolysis behavior in past several decades. Meng et al. [5] synthesized a novel polyimide including 2,6-benzobisoxazole units and determined the actual decomposition reaction mechanisms of this polyimide material by thermogravimetric analysis. It was found that the actual reaction mechanism for the synthesized PI material by the Coats–Redfern method obeyed nucleation and growth model, Avrami–Erofeev function with integral form $g(X) = [-\ln(1 - X)]^3$. Li et al. [6] measured the degradation kinetics of a series of polyimides containing MA, 4,4'-oxydianiline (ODA) and hexafluoroisopropylidene 2,2-bis(phthalic anhydride) (6FDA) by dynamic TGA under nitrogen atmosphere at different heating rates. The apparent activation energies for their thermal degradation were evaluated by iterative iso-conversional procedure, and the mechanism and pre-exponential factor were determined by Coats–Redfern and Achar methods. Lua and Su [7]

✉ Fanglong Zhu
18003868331@163.com

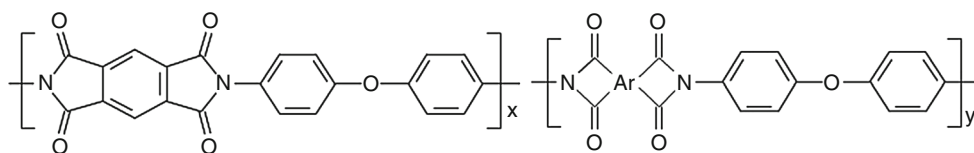
¹ College of Clothing, Zhongyuan University of Technology, Zhengzhou, People's Republic of China

² College of Textile, Donghua University, Shanghai, People's Republic of China

studied the thermal decomposition of Kapton polyimide 100HN under nitrogen atmosphere by applying various fitting techniques with Coats Redfern, Mac Callum Tanner and van Krevelen approaches to the isothermal and non-isothermal gravimetric data. Regnier and Guibe [8] used six kinetic fitting methods including those of Kissinger, Ozawa, Horowitz-Metzger, Coats–Redfern, MacCallum–Tanner and van Krevelen to study the thermal degradation of KERIMID 736 polyimide polymer. Hatori et al. [9] investigated pyrolysis mechanism of Kapton-type polyimide with special attention to the early stage. They used two approaches to reveal the pyrolysis reactions: one is an analysis of evolved compounds; the other is a hydrolysis method that selectively converts polyimide char into low-molecular mass compounds. It was easy to found that the Coats–Redfern method has been used to determine the reaction mechanism of PI pyrolysis. However, Coats–Redfern approach is generally considered unsuitable for determination of kinetic parameters. Model-fitting methods lead to the uncertainty in estimating the activation energy due to uncertainty of choosing the reaction models.

Recently, a novel polyimide material synthesized from 4,4'-oxydianiline(ODA), 1,2,4,5-benzenetetracarboxylic anhydride (PMDA), benzophenonetetracarboxylic acid (BTE) units (Fig. 1) under the trademark YILUN has been developed by Hipolyking Co., Ltd. Changchun, China [10]. The thermal performance of YILUN samples [11, 12] has been reported. These results from thermogravimetric analysis indicated that the thermal decomposition temperature of this fiber was above 500 °C, and the glass transition temperature was about 380 °C. After aged at 280 °C for 100 h in air, it can maintain 80% of the tensile strength. The limited oxygen index (LOI) of the fiber is 38 with good flame retardancy. However, to the best of our knowledge, few papers have reported thermal degradation and combustion characteristics of this kind of polyimide material. Consequently, the present work aimed at documenting the thermal degradation behavior of YILUN short fiber by dynamic TGA under nitrogen atmosphere at different heating rates. The kinetic parameters of degradation were calculated via the Kissinger, Flynn–Wall–Ozawa (FWO) and Kissinger–Akahira–Sunose (KAS) method, and the degrade mechanism was defined using master-plots method. At last, the combustion properties of YILUN short fiber were investigated by MCC tests.

Fig. 1 Molecular structure of (ODA + PMDA + BTDE) YILUN polyimide fiber



Theoretical background

In general, the decomposition of solid polymers can be associated with the formation solid and gaseous products, which can be represented by the process: A solid polymer $\rightarrow B$ solid + C gas. The kinetic parameters were evaluated from non-isothermal experiments. The conversion degree α was determined by using Eq. (1) where W_i , W , and W_f represented the mass of the solid polymer sample recorded at the beginning, at a time t , and after complete degradation, respectively.

$$\alpha = \frac{W_i - W}{W_i - W_f} \quad (1)$$

A typical model for a kinetic process can be expressed as

$$\frac{d\alpha}{dt} = k \cdot f(\alpha) \quad (2)$$

where $\frac{d\alpha}{dt}$ is the decomposition rate, k is the decomposition rate constant, and $f(\alpha)$ depends on the mechanism of the degradation reaction. The function k is usually described by Arrhenius equation

$$k = A \cdot \exp\left(-\frac{E}{RT}\right) \quad (3)$$

where A is the pre-exponential factor (min^{-1}), E is the activation energy (J mol^{-1}), T is the absolute temperature (K), and R is the universal gas constant ($8.314 \text{ J mol}^{-1} \text{ K}^{-1}$).

Kinetics of polymer decomposition may be described as follows

$$\frac{d\alpha}{dT} = \frac{A}{\beta} \cdot \exp\left(-\frac{E}{RT}\right) \cdot f(\alpha) \quad (4)$$

Rearrangement of Eq. (6) and integration of this equation from an initial temperature, T_0 , corresponding to a degree of conversion α_0 , to the peak temperature, T_p , where $\alpha = \alpha_p$, gives the integral form $g(\alpha)$ of the reaction model $f(\alpha)$

$$g(\alpha) = \int_0^{\alpha_p} \frac{d\alpha}{f(\alpha)} = \frac{A}{\beta} \int_0^{T_p} \exp\left(-\frac{E}{RT}\right) dT \quad (5)$$

As far as polymer is concerned, the integral function $g(\alpha)$ is a sigmoidal type function or a reduction function. Table 1 lists different solid-state reaction mechanism functions $f(\alpha)$ and $g(\alpha)$ [13]. These functions can be used to

Table 1 Algebraic expressions for the kinetics models $f(\alpha)$ and $g(\alpha)$ for the kinetic mechanisms of solid-state processes

Kinetic mechanism	Kinetic model	
	$f(\alpha)$	$g(\alpha)$
Reaction order (random nucleation)		
F1: first-order random nu	$1 - \alpha$	$-\ln(1 - \alpha)$
F2:	$(1 - \alpha)^2$	$1/(1 - \alpha)^{-1}$
F3:	$(1 - \alpha)^3/2$	$1/(1 - \alpha)^2 - 1$
Diffusion (Dn)		
D1:	$1/(2\alpha)$	α^2
D2:	$[-\ln(1 - \alpha)]^{-1}$	$(1 - \alpha) \ln(1 - \alpha) + \alpha$
D3:	$3/2(1 - \alpha)^{2/3}[1 - (1 - \alpha)^{1/3}]^{-1}$	$[1 - (1 - \alpha)^{1/3}]^2$
D4:	$3/2[(1 - \alpha)^{-1/3} - 1]$	$1 - 2\alpha/3 - (1 - \alpha)^{2/3}$
Nucleation and growth (An)		
A2:	$2(1 - \alpha)[- \ln(1 - \alpha)]^{1/2}$	$[- \ln(1 - \alpha)]^{1/2}$
A3:	$3(1 - \alpha)[- \ln(1 - \alpha)]^{2/3}$	$[- \ln(1 - \alpha)]^{1/3}$
A4:	$4(1 - \alpha)[- \ln(1 - \alpha)]^{3/4}$	$[- \ln(1 - \alpha)]^{1/4}$
Phase boundary controlled reaction		
R1: one-dimensional movement	1	α
R2: Contracting area	$2(1 - \alpha)^{1/2}$	$1 - (1 - \alpha)^{1/2}$
R3: Contracting volume	$3(1 - \alpha)^{2/3}$	$1 - (1 - \alpha)^{1/3}$

speculate the solid-state reaction mechanism from non-isothermal TG experiments.

Kissinger method

The method has the advantage that it does not require previous knowledge of the reaction mechanisms to determine activation energy. First reported by Kissinger in 1957 [14], this method developed a model-free non-isothermal method where is no need to calculate activation energy E for each conversion value in order to evaluate kinetic parameters. This method is based on the fact the reaction rate $d\alpha/dt$ will rise to a maximum value with an increase in reaction temperature. Activation energy E is obtained from the slope of $\ln(\beta/T_m^2)$ against $1000/T_m$ for a series of experiments at different heating rate (β), where T_m is the temperature peak of DTG curve. The equation can be obtained as follow

$$\ln\left(\frac{\beta}{T_m^2}\right) = \ln\left(\frac{AR}{E}\right) - \frac{E}{RT_m} \tag{6}$$

The activation energy E can be calculated from the slope of the plot, which is equal to $-E/R$.

FWO method

Flynn–Wall–Ozawa (FWO) method is one of the integral methods that can determine the activation energy without pre-knowledge of reaction mechanism and differential data of TGA [15, 16]. It is usual to assume that the rate of decomposition $d\alpha/dt$ is proportional to the mass quotient of the un-reacted material. The FWO method is based on the Doyle approach [17] for the integral which allows $(\ln p(E/RT)) \cong -2.315 - 0.4567E/RT$. Substituting Doyle’s approximation into Eq. (5) results in

$$\log \beta = \log \frac{AR}{Rg(\alpha)} - 2.315 - 0.4567 \frac{E}{RT} \tag{7}$$

For a constant conversion, a plot of $\ln \beta$ versus $1/T$, from the data at different heating rates, leads to a straight line whose slope provides E calculation.

Kissinger–Akahira–Sunose method (KAS)

The KAS method is one of the most commonly accepted methods for the computation of the kinetic parameters, based on thermogravimetric analyses. By introducing the approximation $p(E/RT) \cong \exp(-E/RT)/(E/RT)^2$ into Eq. (6) [18], the relation between heating rate and inverse temperature becomes

$$\ln \frac{\beta}{T^2} = \ln \frac{AR}{Eg(\alpha)} \quad (8)$$

The apparent activation energy can be obtained from the slope of the linear plot of $\ln(\beta/T^2)$ against $1000/T$ for each value of conversion, where the slope equals to E/R .

Z(α) Master-plot method

The master-plot method defined by Criado determines the kinetic mechanism based on the comparison of an experimental function $Z(\alpha)$, obtained from exponential factor A and activation energy E , with master curves obtained from theoretical kinetic models $f(\alpha)$ and $g(\alpha)$ (Table 1) [19]. The $Z(\alpha)$ plot derived by combined the integral and differential forms of reaction model is given as follows

$$Z(\alpha) = f(\alpha) \cdot g(\alpha) \quad (9)$$

The experimental $Z(\alpha)$ function can be obtained from Eq. (14) by combined Eqs. (4) and (5)

$$Z(\alpha) = \frac{d\alpha}{dt} \cdot \frac{T}{\beta} \pi(\chi) \quad (10)$$

Because the exponential integral has no analytical solution, a fourth rational expression of Senum–Yang approximation was given [20]. By plotting $Z(\alpha)$ against α corresponding to different kinetic model functions, the theoretical master plots can be obtained for various kinetic mechanisms. Simultaneously, the experimental master plots can be also drawn from experimental data for different heating rates. The theoretical and experimental $Z(\alpha)$ curves are compared, and the best fitting model is determined.

Table 2 Technical parameters of polyimide short fiber used in this study

Item	Unit	Technical
Fineness	dtex	1.67
Length	mm	51
Breakdown strength	cN/dtex	> 4
Elongation at break	%	> 20
Dry thermal shrinkage rate	%	< 0.3
Limited oxygen index (LOI)	%	38
Thermal conductivity	W/(m k)	0.03

Experimental work

Material

The polyimide short fibers 51 mm in length (Trade name Yilun[®]) used for this study were obtained from Hipolyking Co., Ltd. Changchun, China. The detailed technical parameters for this kind of fiber are shown in Table 2. The sample was washed and dried in a dry oven with 80 °C. Then, the dried sample was ground to a particle size range of 0.5 mm.

Thermal analysis tests

Thermogravimetric analysis was performed using Netzsch TG209-F1 thermal analyzer, operated in the dynamic mode in a dry nitrogen atmosphere flowing at 25 mL min⁻¹ from 20 to 800 °C. Fiber samples of average particle size of 50–100 μ m were taken in alumina crucibles with samples of 5 mg. These experiments were performed at four nominal heating rates of 5, 10, 20, 40 K min⁻¹.

FTIR measurements

Transmission FTIR spectra of the polyimide fibers were obtained in a Tensor 37 spectrometer (Bruker, Germany). A resolution of 2 cm⁻¹ and 32 scans per file was used. All virgin and pyrolyzed samples were cold-ground at 77 K in a mixer mill used in combination with a cooling attachment where liquid nitrogen was the coolant.

MCC measurement

In this paper, the flammability of PI fiber was evaluated by MCC tests, which were conducted using a FTT0001 microscale combustion calorimeter produced by British. The sample, approximate 5 mg, was heated from 75 to 750 °C using a linear heating rate (1 °C s⁻¹) in a mixture stream of nitrogen flowing at 80 cm³ min⁻¹ flow rate and oxygen flowing at 20 cm³ min⁻¹.

Results and discussion

Analysis of TG and DTG curves

Thermogravimetric (TG) curves showing changes in sample mass with temperature during pyrolysis at different heating rates under non-isothermal conditions are shown in Fig. 2. Table 3 lists the values of the onset decomposition temperature $T_{5\%}$ (the temperature at the mass loss of 5%), the extrapolated initial temperature T_{ini} , the maximum

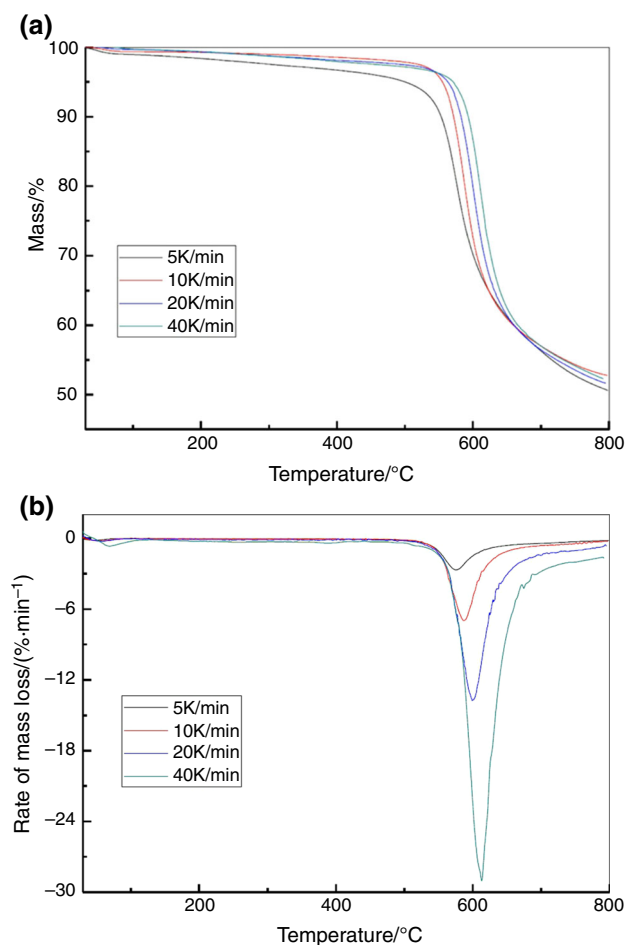


Fig. 2 TG (a) and DTG (b) curves of PI fiber during non-isothermal pyrolysis

Table 3 Temperatures and Char yield at 800 °C under different heating rates

Heating rate/°C min ⁻¹	T _{5%} /°C	T _{ini} /°C	T _{max} /°C	Char
5	500.2	548.1	575.6	50.8
10	554.8	562.0	586.9	52.7
20	562.8	574.1	600.9	50.9
40	571.0	585.5	613.2	52.1

decomposition temperature T_{\max} (the temperature at maximum mass loss rate), and the char residues (at 800 °C).

It can be clearly seen from Fig. 2 and Table 3 that the decomposition reaction depended on the heating rate, and the DTG profiles were shifted to slightly high temperatures at higher heating rates. This phenomenon can be explained by that the higher temperatures gradient developed between the temperatures of the TG furnace and the sample, and thermal lag occurred with the increase in the heating rate. At a given temperature, a higher heating rate

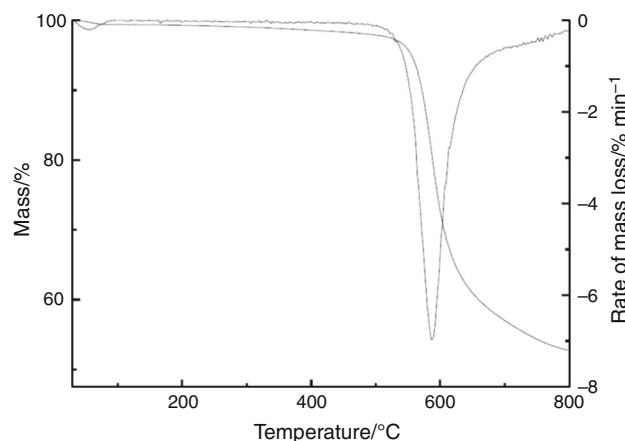


Fig. 3 Typical TG-DTG curves of PI fiber at a heating rate of 10 K/min

implies that the material reaches the given temperature in a shorter time and there is not enough time to decompose. All these TG curves showed the same features. Simultaneously, at the end of the degradation (800 °C) about 51% residues remained. From the kinetics point of view, the thermal decomposition behavior suggested that the reaction rate was only function of the temperature and was independent of the heating rates. Similar phenomena could be observed from other polyimide materials [5–7]. Therefore, an intermediate heating rate of 10 K min⁻¹ was chosen as an example to probe into the subsequent thermal degradation process.

TG and DTG curves obtained during polyimide fiber pyrolysis under N₂ atmosphere with a heating rate of 10 K min⁻¹ are presented in Fig. 3. The small humps below 100 °C in the DTG curve were due to the loss of moisture from the fiber. The decomposition of YILUN short fiber started at about 504 °C and the sample mass decreased significantly within a narrow temperature range of 550 and 650 °C with the evolution of mainly CO and CO₂ as gaseous products. The high onset decomposition temperature and char residues (about 52%) illustrated that the polyimide material had excellent stability. The mass loss in the pyrolysis stage showed that polyimide degradation occurred in single-step process at the main decomposition stage, as could be concluded by the presence of one distinct exothermic peak in DTG curve. This was attributed to the decomposition of the imide segment rupture.

FTIR analysis

The FTIR spectra of virgin fiber and the samples treated at temperature 500–800 °C are shown in Fig. 4. The infrared spectrogram involved 6 spectra corresponding to different pyrolyzed temperatures. In the thermal decomposition process, the polyimide fiber released the SO₂, NO₂, HCN,

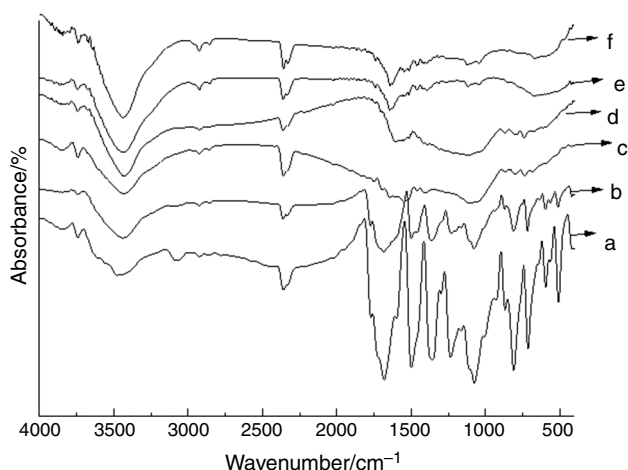


Fig. 4 FTIR spectra of virgin YILUN (a) and its solid decomposition products at 500 °C (b), 600 °C (c), 650 °C (d), 700 °C (e), and 800 °C (f)

NH_3 , NO, CO, CO_2 , and H_2O molecules [12]. The rigid nature of its diimide moiety (PMDA) and aromatic heterocyclic ring (Ar) result in the poor solubility of the polyimide fiber, which was not soluble in conventional polar aprotic solvents, such as MEK, DMF, NMP, DMAc, and DMSO. The characteristic absorption peaks of amide and carboxyl disappearance indicated that the polyamic acid (PAA) precursor converted into the polyimide completely. For the virgin polyimide fiber, the following band assignments can be made: the wide absorption peak at a near 3440 cm^{-1} (N–H and O–H stretching vibration of imide and hydroxyl end group), 3100 cm^{-1} (C–H stretching vibration of the benzene ring between the Ar aromatic heterocyclic ring), 2362 cm^{-1} (the peak of C=O), 1683 cm^{-1} (C=O stretching), 1499 cm^{-1} (skeletal vibrations of the conjugated system), 1365 cm^{-1} (C–N stretching), 1250 cm^{-1} (C–C stretching), 1079 cm^{-1} (imide ring deformation), 813 cm^{-1} (symmetric C–O–C stretching of a cyclic ether from ODA moiety), 719, 599 and 514 cm^{-1} (out-of-plane C–H vibrations of aromatic rings). The

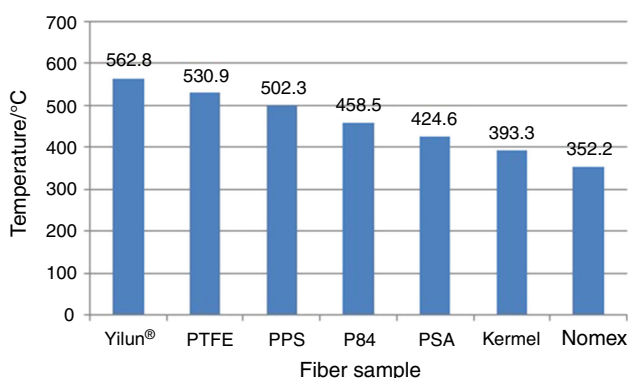


Fig. 5 Comparisons of decomposition temperature of 5% mass loss for different flame resistant fibers

sample heated to 500 °C had virtually the same trend band as that of the virgin fiber. This implied that the decomposition started at a temperature above 500 °C, corresponding to temperatures at 5% mass loss in nitrogen. At the same time, YILUN short fiber exhibited better thermal stability than that of other inherently flame resistant fibers, such as PTFE, PPS, P84, PSA, Kermel, and Nomex fiber. The decomposition temperatures of $T_{5\%}$ for these fibers are presented in Fig. 5 [11]. It can be validated from the comparisons, and the polyimide fiber (YILUN fiber) has the highest decomposition temperature of $T_{5\%}$ among these inherently flame resistant fibers. At 600 °C (Fig. 4c), great changes in the FTIR spectra occurred and the initial band were severely altered. Above 700 °C (Fig. 4e), all the bands ascribed to the imide group, ODA moiety (C–O–C) disappeared completely. In contrast, the band for C=O stretching (1683 cm^{-1}) persisted and even broadened with increasing pyrolyzed temperature.

Calculation of activation energy

The results obtained from the thermo-gravimetric analysis are illuminated according to model-free methods to calculate the kinetic parameters. The activation energy (E) values were calculated by using Kissinger, KAS, and FWO methods. Firstly, the kinetic parameters for the polyimide fiber were calculated using the Kissinger method. The maximum temperature T_m corresponding to the maximum mass peaks at four different heating rates was obtained from DTG curves which are shown in Fig. 2b. $\ln(\beta/T_m)$ was then plotted against $1/T$ of decomposition process for the fiber (Fig. 6a). The regression equations and the correlation coefficient (R) are also presented. The linearity of the relationship was good, demonstrating a close fit for the proposed model. The activation energy value determined from the slope and intercept of the fitting linear line (Fig. 6a) was $355.86\text{ kJ mol}^{-1}$.

According to KAS model, activation energy E based on Eq. (11) can be determined from a plot of $\ln(\beta/T^2)$ versus $1000/T$ where slopes give $(-E/R)$ at progressing conversion degrees (Fig. 6c). Kinetic data have been also calculated by using the FWO method (Fig. 6b). Once again from the linear plots of $\log\beta$ versus the inverse temperature $1000/T$, the activation energies of each value of conversion can be obtained from the slope of the curves. These calculated values from KAS and FWO methods are listed in Table 4. These results indicated that the activation energy values obtained from FWO and KAS method were in good agreement. This agreement validated the reliability of calculations and confirmed the predictive power of FWO and KAS methods [21]. Because the average values of activation energy worked out by the FWO and KAS

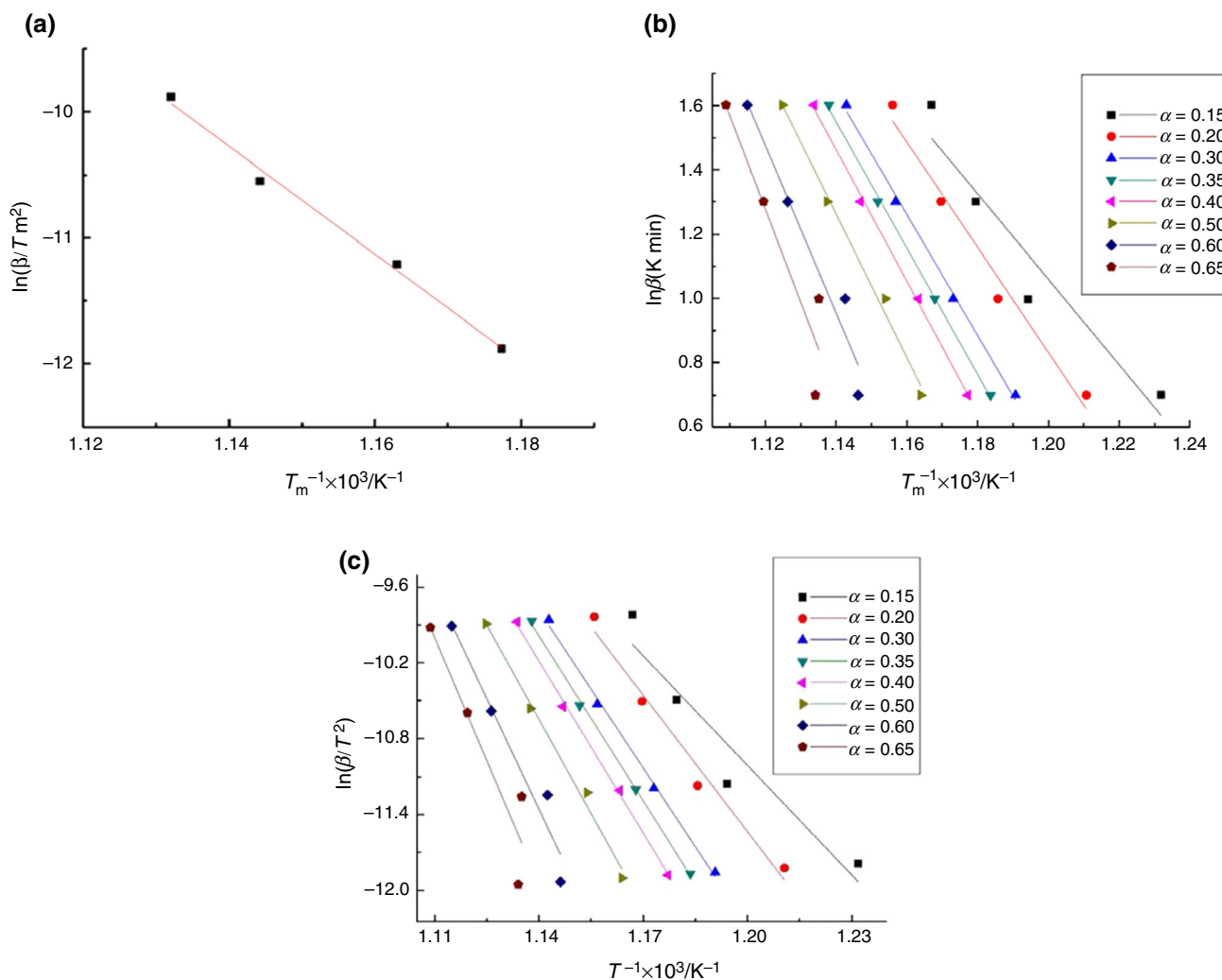


Fig. 6 Plots for the identification of activation energies during PI degradation at different heating rates using Kissinger (a), FWO (b), and KAS (c) methods

Table 4 Activation obtained at different conversion rates

Conversion rate/ α	FWO method		KAS method	
	$E/$ kJ mol^{-1}	Linear correlation coefficient, R	$E/$ kJ mol^{-1}	Linear correlation coefficient, R
0.15	241.85	0.9419	240.41	0.9355
0.20	297.77	0.9844	299.31	0.9829
0.30	342.48	0.9979	345.62	0.9978
0.35	357.48	0.9991	361.86	0.9991
0.40	372.35	0.9987	377.27	0.9987
0.50	406.41	0.9944	413.16	0.9938
0.60	474.08	0.9639	484.19	0.9621
0.65	526.66	0.9046	539.14	0.9003
Average	377.39		382.62	

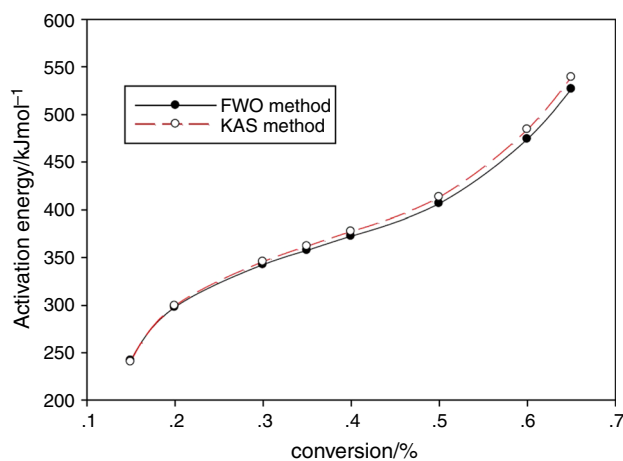


Fig. 7 Change in activation energy with progressing conversion for FWO and KAS methods

method were very close, the average value of two methods ($380.01 \text{ kJ mol}^{-1}$) was chosen as the value of activation energy used in the further study. However, the activation energy was highly dependent on conversion degrees and increased from 0.15 to 0.65. Figure 7 depicts change in activation energy with progressing conversions. In general, activation energy is the minimum energy required to start a chemical reaction; therefore, higher E values mean slower reactions. Activation energy E can be also used for evaluation of thermal stability of polyimide material. Higher E values imply excellent thermal stability. The calculated E average value for YILUN fiber ($380.01 \text{ kJ mol}^{-1}$) was similar with that ($361.36 \text{ kJ mol}^{-1}$) of polyimide containing 2,6-benzobisoxazole units [5].

Determination of the most probable kinetic mechanism

To obtain the prime kinetic expression, we have used the method proposed by Criado. This method uses reference theoretical curves called master plots, which are compared to experimental data. Figure 8 shows the plots of the experimental $Z(\alpha)$ convolution function superimposed on the master curves obtained from theoretical kinetic models of thermal degradation of polyimide materials performed at a heating rate of 10 K min^{-1} . Plots obtained at other heating rate showed the same behavior. Because the Doyle approximation had been used, only conversion values in the range of 5–20% were considered for discussion. As can be seen, the experimental curve of PI nearly overlaps the master curve $Z(\text{F3})$, indicating that the thermal degradation of PI belonged to F3 reaction mechanism. Therefore, the mechanism expression F3 can be determined as the most probable kinetic reaction mechanism.

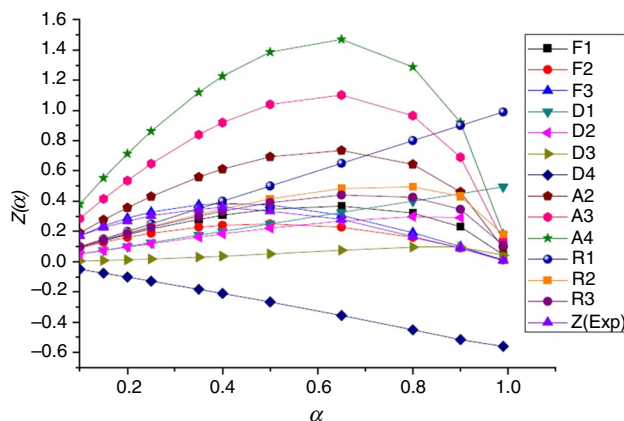


Fig. 8 Plots of experimental $Z(\alpha)$ convolution function superimposed on master on curves of theoretical kinetic model for pyrolysis of PI fiber at the heating rate of 10 K min^{-1}

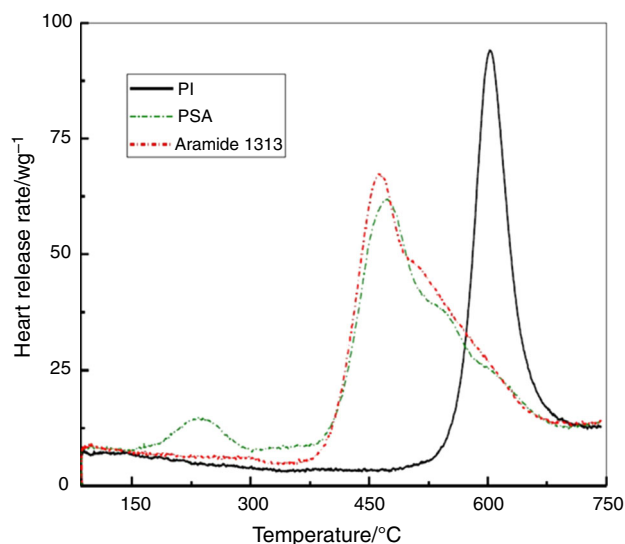


Fig. 9 Heat release rate versus temperature curves of the PI fiber

Table 5 Typical data obtained from MCC

Sample	HRC/ $\text{J g}^{-1} \text{ K}^{-1}$	PHRR/ W g^{-1}	THR/ kJ g^{-1}	$T_{\text{pHRR}}/$ $^{\circ}\text{C}$	LOI/ %
PI	93.00	83.69	4.50	602.20	38
PSA	59.00	50.92	8.50	461.20	33
Aramid 1313	62.00	55.43	7.10	455.50	29

Flammability performance

The MCC is an effective microscale testing method for evaluating the combustion properties and the fire hazard of a polymer material. The parameters used to characterize flammability examined by using MCC are heat release rate (HRR), peak heat release rate (PHRR), total heat release (THR), temperature at PHRR (T_{p}), heat release capacity (HRC) and percentage of residue char. Figure 9 describes the HRR curves of different fibers, and relevant combustion data are listed in Table 5. The HRR versus temperature curve for PI fiber showed that PI material started degradation at about 500°C , and the degradation quickly reaches its peak with PHRR of 83.69 W g^{-1} . PI fiber had highest PHRR among these three inherently flame-retardant fibers. However, the PHRR peak of PI fiber was much narrower than those of PSA and NOMEX fiber. These phenomena denoted that thermal oxidative degradation temperature interval for PI fiber was much narrower than those of the other two kinds of fibers. These results can be read from these narrowest and longest heat release curve for PI fiber (Fig. 9). The THR value can be achieved by the temperature integral for the curve. Therefore, the THR

value (4.50 kJ g^{-1}) of PI fiber was lowest among these three kinds of fibers. Observed from the LOI data, PI's higher LOI value than PSA and meta-aramid suggested that it had lowest flammability in terms of the ability to ignite among these fibers. However, the HRC and PHRR of PI were higher than PSA and meta-aramid, demonstrating higher flammability in terms of the amount of heat they releases during combustion [20]. Compared with the PSA and Nomex 1313 fibers, PI fiber thermal decomposed at the highest temperature ($602.20 \text{ }^\circ\text{C}$) with fastest heat release rate and yielded highest percentage of char at the end. The characteristic temperatures of thermal decomposition were consistent with the TG (DTG) results. These results displayed that the prepared PI fiber exhibited more excellent thermal stability than the other two kinds of flame-retardant fibers.

Conclusions

In this study, the pyrolysis of polyimide material containing ODA, PMDA, and BTDE units has been investigated first time by means of thermo-gravimetric analysis under nitrogen conditions and operated at different heating rates of 5, 10, 20, and 40 K min^{-1} . The activation energy calculated by Kissinger method was 355.86 kJ/mol , and the mean value of activation energies obtained from FWO and KAS methods were 377.39 and $382.62 \text{ kJ mol}^{-1}$. The result of kinetic analysis through Master-plot methods suggested that the thermal degradation stage of this novel synthesized PI material can be described by the random nucleation equation ($1/(1 - \alpha)^2 - 1$). From the view of flammability, it was found that PI materials possessed poor ability to ignite, but compared with other inherently flame-retardant fibers (PSA and Nomex 1313 fibers), they had higher HRC and pHRR during combustion. The experimental results and kinetics parameters provided useful information for the understanding of mechanism and the numerical simulation of pyrolysis process of newly prepared PI materials.

Acknowledgements This study was financially supported by the National Natural Science Foundation of China (51576215, U130543) and the National Key Research and Development Program of China (2017YFB0309000).

References

1. Wang QN, Bai YY, Xie JF. Synthesis and filtration properties of polyimide nanofiber membrane/carbon woven fabric sandwiched hot gas filters for removal of PM_{2.5} particles. *Powder Technol.* 2016;292:54–63.
2. Morgan AB, Putthanarat S. Use of inorganic materials to enhance thermal stability and flammability behavior of a polyimide. *Polym Degrad Stab.* 2011;96:23–32.
3. Cai GM, et al. Experimental investigation on the thermal protective performance of nonwoven fabrics made of high-performance fibers. *J Therm Anal Calorim.* 2015;121:627–32.
4. Udayraj, Talukdar P, Das A, Alagirusamy R. Estimation of radiative properties of thermal protective clothing. *Applied Thermal Engineering.* 2016; 100:788–797.
5. Meng XL, Huang YD, Yu H, Lv ZS. Thermal degradation kinetics of polyimide containing 2,6-benzobisoxazole units. *Polym Degrad Stab.* 2007;92:962–7.
6. Li LQ, et al. Thermal stabilities and thermal degradation kinetics of polyimide. *Polym Degrad Stab.* 2004;84:369–71.
7. Lua AC, Su J. Isothermal and non-isothermal pyrolysis kinetics of Kapton[®] polyimide. *Polym Degrad Stab.* 2004;91:144–53.
8. Regnier N, Guibe C. Methodology for multistage degradation of polyimide polymer. *Polym Degrad Stab.* 1997;55:165–72.
9. Hatori H, et al. The mechanism of polyimide pyrolysis in the early stage. *Carbon.* 1996;34:201–8.
10. Polyimide short fiber, <http://www.hipolyking.com/fiber.asp?id=3&tid=1>. (date of access: 8/3/2016).
11. Sun F, et al. Study on the thermal stability of polyimide fiber YILUN. *Synth Fiber China.* 2012;41:6–9.
12. Yang JJ, et al. The properties and application YILUN polyimide short fiber. *Hi Tech Fiber Appl.* 2012;37:57–60.
13. Vyazovkin S, Wight CA. Kinetics in solids. *Annu Rev Phys Chem.* 1997;48:125–49.
14. Kissinger H. Variation of peak temperature with heating rate in differential thermal analysis. *J Res Nat Bur Stand.* 1956;57:217–21.
15. Ozawa T. A new method of analyzing thermogravimetric data. *Bull Chem Soc Jpn.* 1965;38:1881e6.
16. Flynn JH, Wall LA. A quick, direct method for the determination of activation energy from thermogravimetric data. *Polym Lett.* 1966;4:323–8.
17. Doyle CD. Series approximation to the equation of thermogravimetric data. *Nature.* 1965;207:290–1.
18. Kissinger HE. Reaction kinetics in differential thermal analysis. *Anal Chem.* 1957;29:1702–6.
19. Criado JM, Malek J, Orgega A. Applicability of the master plots in kinetic analysis of non-isothermal data. *Thermochim Acta.* 1989;147:377–85.
20. Vyazovkin SV, Lesnikovich AI. An approach to the solution of the inverse kinetic problem in the case of complex processes: part 1. Methods employing a series of thermoanalytical curves. *Thermochim Acta.* 1990;165:272–80.
21. Yang CQ, He QL, Lyon RE, Hu Y. Investigation of the flammability of different textile fabrics using micro-scale combustion calorimetry. *Polym Degrad Stab.* 2010;95:108–15.